

# PMMA-Multigraft Copolymers Derived from Linseed Oil, Soybean Oil, and Linoleic Acid: Protein Adsorption and Bacterial Adherence

Birten Çakmaklı,<sup>1</sup> Baki Hazer,<sup>1</sup> Şerefden Açıkgöz,<sup>2</sup> Murat Can,<sup>2</sup> Füsün B. Cömert<sup>3</sup>

<sup>1</sup>Department of Chemistry, Faculty of Arts and Sciences, Zonguldak Karaelmas University, 67100 Zonguldak, Turkey

<sup>2</sup>Department of Biochemistry, Faculty of Medicine, Zonguldak Karaelmas University, 67100 Zonguldak, Turkey

<sup>3</sup>Department of Microbiology, Faculty of Medicine, Zonguldak Karaelmas University, 67100 Zonguldak, Turkey

Received 11 August 2006; accepted 18 February 2007

DOI 10.1002/app.26397

Published online 30 May 2007 in Wiley InterScience (www.interscience.wiley.com).

**ABSTRACT:** Synthesis of Poly(methyl methacrylate), PMMA-multigraft copolymers derived from linseed oil, soybean oil, and linoleic acid PMMA-*g*-polymeric oil/oily acid-*g*-poly(3-hydroxy alkanooate) (PHA), and their protein adsorption and bacterial adherence have been described. Polymeric oil/oily acid peroxides [polymeric soybean oil peroxide (PSB), polymeric linseed oil peroxide (PLO), and polymeric linoleic acid peroxide (PLina)] initiated the copolymerization of MMA and unsaturated PHA-soya to yield PMMA-PLO-PHA, PMMA-PSB-PHA, and PMMA-PLina-PHA multigraft copolymers. PMMA-PLina-PHA multigraft copolymers were completely soluble while PMMA-PSB-PHA and PMMA-PLO-PHA multigraft copolymers were partially crosslinked. Crosslinked parts of the PLO- and PSB-multigraft copolymers were isolated by the sol gel analysis and characterized by swelling measurements in CHCl<sub>3</sub>. Soluble part of the PLO- and PSB-multigraft copolymers and completely soluble PLina-multigraft copolymers were obtained and characterized by spectro-

scopic, thermal, gel permeation chromatography (GPC), and scanning electron microscopy (SEM) techniques. In the mechanical properties of the PHA-PLina-PMMA, the elongation at break is reduced up to ~ 9%, more or less preserving the high stress values at its break point (48%) when compared to PLina-*g*-PMMA. The solvent casting film surfaces were studied by means of adsorption of blood proteins and bacterial adhesion. Insertion of the PHA into the multigraft copolymers caused the dramatic increase in bacterial adhesion on the polymer surfaces. PHA insertion into the graft copolymers also increased the protein adsorption. © 2007 Wiley Periodicals, Inc. *J Appl Polym Sci* 105: 3448–3457, 2007

**Key words:** poly (3-hydroxyalkanoate)s; PHA-soya; *Pseudomonas oleovorans*; autooxidation; polymeric linseed oil; polymeric soy bean oil; polymeric linoleic acid; stress-strain behavior; blood compatibility; bacterial adherence

## INTRODUCTION

Many microorganisms produce polyesters as energy reserve material from a wide variety of carbon substrates,<sup>1–3</sup> including alkanes, alcohols, alkenes, alkanolic acids, and their derivatives.<sup>4–11</sup> Unsaturated hydrophobic PHAs are produced by *Pseudomonas oleovorans* from edible oils such as soya bean and linseed oil,<sup>12–16</sup> which are sticky, waxy, and soft materials. Chemical modification technique is used to improve the mechanical and viscoelastic properties of the PHAs.<sup>17–19</sup> Unsaturated PHA obtained from soy bean oil (PHA-soya) was grafted with poly(ethylene glycol) (PEG)<sup>20</sup> and PMMA<sup>21,22</sup> in our laboratories. Recently, considerable research has been concentrated on the

development of bio-based polymers using natural oils or their derivatives as the main comonomer. Wool et al. and Aranguren et al. have, respectively, developed a series of polymer resins using multifunctional soybean and linseed oil derivatives as a main component and styrene as a comonomer.<sup>23</sup> In addition, peroxidized linoleic acid polymer is a member of polymeric peroxides<sup>24,25</sup> and therefore can lead to multi-block copolymer.<sup>26</sup>

On the other hand, we have recently reported the autooxidation of the unsaturated edible aliphatic oils such as linseed oil (LO), soy bean oil (SB), and linoleic acid (Lina) to prepare polymeric oil peroxy initiators (PLO, PSB, and PLina)<sup>27–29</sup> for free radical polymerization.

Tissue engineering uses polymer materials, including pure polymers such as PMMA, polymer blends, and copolymers as biomedical materials.<sup>30</sup> The biocompatibility of a polymer material can be inferred by studying the protein adsorption on this polymer. When a polymer is implanted, the first body reaction is protein adsorption. The adsorbed proteins determine later body reactions and finally determine

Correspondence to: B. Çakmaklı (bicakmakli@yahoo.com).

Contract grant sponsor: Zonguldak Karaelmas University Research Fund; contract grant number: 2004-13-02-01.

Contract grant sponsor: TÜBİTAK research project; contract grant number: 104M128.

whether the material is accepted or rejected by the body. Surface chemical structures as well as surface morphology can mediate protein adsorption behavior.<sup>31</sup> Protein adsorption is a complex process involving van der Waals, hydrophobic and electrostatic interactions, and hydrogen bonding. The purification of albumin is generally required for the treatment of hypoproteinemia. Hydrophobic interaction separation has become a popular technique for purifying proteins and enzymes.<sup>32,33</sup>

Synthetic materials used in blood-contacting devices suffer from poor hemocompatibility. To solve this problem, better knowledge of the mechanisms of blood interaction with materials is necessary. A principal mechanism is the adsorption of plasma proteins. When blood first comes into contact with foreign materials, plasma proteins are adsorbed onto the surfaces in less than a second. The adsorption of proteins affects subsequent platelet adhesion, which plays a major role in thrombogenesis on foreign surfaces.<sup>34</sup>

Human albumin,  $\gamma$ -globulin, and fibrinogen were used as model proteins to study the surface adsorption of proteins. Protein adsorption onto polymer surfaces is important because of its possible involvement at the initial stage of blood coagulation. Albumin is the major constituent of blood plasma (representing about 60% of plasma proteins) and is also one of the smallest proteins in the plasma. As a fibrinogen molecule adsorbs on a polymer surface, it undergoes structural, conformational, or orientational changes. Such changes greatly affect the binding capability of fibrinogen molecules to platelets. The surface-bound fibrinogen has an important role in thrombus formation. Therefore, understanding the molecular structures of fibrinogen molecules adsorbed on different surfaces should contribute to the understanding of platelet adhesion on such surfaces and thus the blood compatibility of these material.<sup>31–35</sup>

Bacteria and other microorganisms have a natural tendency to adhere to surfaces as a survival mechanism. This can occur in many environments including the living host, industrial systems, and natural waters. The general outcome of bacterial colonization of surfaces is the formation of an adherent layer (biofilm) composed of bacteria embedded in an organic matrix.<sup>36</sup> In many biomedical applications the adhesion of bacteria to biomaterials causes undesirable inflammation or infection. In recent years, various groups have therefore focused on the development of bioinert, biocompatible coatings that can be used to minimize protein adsorption and bacterial adhesion while maintaining the mechanical and physical properties of the underlying substrate.<sup>37</sup>

Polymeric materials, including pure polymers and copolymers, are extensively applied as biomedical materials. The biocompatibility of a polymeric material is important in biomedical applications such as

blood-contacting devices. Our recent studies have been focused on the diversification of the biomedical polymers. In this manner, this work refers to the synthesis of some new types of biodegradable polymer materials-graft copolymers containing PHA-soya, polymeric oil/oily acid, and PMMA, at a low temperature with tetraethylene pentamine as a catalyst.

## EXPERIMENTAL SECTION

### Materials

Linseed oil was supplied from Aldrich (St. Louis, MO), soybean oil was locally supplied and both were used as received. Linseed oil and soybean oil are triglycerides and they contain linoleic acid of 15.3 and 51 mol %, respectively.<sup>38</sup>

Linoleic acid (*cis-cis*-9-12-octadecadienoic acid) was supplied by Fluka (Steinheim, Germany), tetraethylene pentamine was obtained from Merck (Darmstadt, Germany) and both were used as received. MMA was supplied by Aldrich and freed from inhibitor by vacuum distillation over  $\text{CaH}_2$ .

Human albumin and  $\gamma$ -globulin were supplied by Sigma and fibrinogen was from Fluka.

All other chemicals were reagent grade and used as received.

### Substrates and PHA biosynthesis

#### Biosynthesis of the PHA-soya

Soybean oil was extracted from the related products grown in Turkey, and hydrolyzed<sup>13</sup> into its fatty acids to make them soluble in water. The acids obtained from the hydrolysis of soybean oil included both saturated (palmitic and stearic: 18 mol %) and unsaturated acids (oleic: 18–26 mol %, linoleic: 50–55 mol %, and linolenic: 7–10 mol %).<sup>38,39</sup> Stock cultures of *P. oleovorans* (ATCC 29347) were used in all growth and polymer production experiments. *P. oleovorans* was grown on soybean oily acid substrate and the resulting polymer was extracted by using methods in Refs. <sup>4–6,13</sup>.

### Autooxidation of the LO, SB, and Lina

For the formation of PLO,<sup>27</sup> PSB,<sup>28</sup> and PLina,<sup>29</sup> 5.0 g of the oil or the oily acid was spread out in a Petri dish ( $\phi = 16$  cm) and exposed to sunlight in the air at room temperature. The upper layer gel film of the PLO, PSB, and PLina were removed by peeling off the gel film layers on these glass plates at the end of specified time intervals (60 days). The lower parts of the gel layers were soluble polymeric oil peroxides: sPLO and sPSB, which are pink-yellow colored viscous liquids. Unlike PLO and PSB, there was no gel layer for PLina, totally pink viscous soluble liquid was observed. The polymeric oil peroxides were characterized by means

**TABLE I**  
Characterization of the Polymeric Oil Peroxides

Polymeric oil peroxide	Peroxygen analysis (wt %)	GPC analysis	
		$M_w$	MWD
sPLO	1.3	2100	1.92
sPSB	1.1	4590	1.52
PLina	0.7	1684	1.22

of gel permeation chromatography (GPC) and peroxygen analysis and then used in the polymerization of MMA with the presence of PHA-soya. Molecular weights of the polymeric oils/oily acid are listed in Table I.

### Peroxygen analysis

Peroxide analysis of polymeric oil/oily acid peroxides was carried out by refluxing a mixture of 2-propanol (50 mL), acetic acid (10 mL), saturated aqueous solution of KI (1 mL), and 0.1 g of the polymeric sample for 10 min and titrating the released iodine against thiosulfate solution according to the literature.<sup>24</sup> Peroxygen contents of the samples varied from 0.66 to 1.32 wt %. Peroxide contents of the polymeric oil/oily acids are listed in Table I.

### Grafting reactions

For grafting reaction, a given amount of a polymeric oil/oily acid, PHA, MMA, and tetraethylene pentamine catalyst were charged separately into a pyrex tube. Argon was introduced through a needle into the tube for about 3 min to expel the air. The tightly capped tube was then put in a water bath at 26°C. After the required time period, the contents of the tube were coagulated in methanol. The graft copolymer samples were dried overnight under vacuum at 30°C. The results and conditions of the grafting reactions are listed in Table II.

### Purification of the graft copolymers

In a typical purification procedure via fractional precipitation,<sup>40,41</sup> 0.5 g of polymer sample was dissolved

in 10 mL of CHCl<sub>3</sub>. Methanol was used as a nonsolvent and kept in a 50-mL buret. Afterwards, methanol was added to the polymer solution with continuous stirring, until the polymer began to precipitate. At this point,  $\gamma$ -value was calculated by taking the volume ratio of the consumed nonsolvent (methanol) to CHCl<sub>3</sub> solution of the graft copolymer. The fractionated polymer was dried under vacuum at room temperature.

### Polymer characterization

<sup>1</sup>H NMR were recorded in CDCl<sub>3</sub> at 17°C with tetramethylsilane as internal standard, using a 400 MHz NMR AC 400 L. A typical <sup>1</sup>H NMR spectra of a multigraft copolymer and its diblock/graft copolymer are given in Figure 1.

Molecular weights of the polymeric samples are determined using GPC with a Waters model 6000A solvent delivery system with a model 401 refractive index detector, a mode 730 data module and two Ultrastaygel linear columns in series. Tetrahydrofuran was used in the elution at a flow rate of 1.0 mL min<sup>-1</sup>. A calibration curve was generated with six polystyrene standards. Figure 2 shows GPC curves of the multigraft copolymers. GPC results of the multigraft copolymers are listed in Table III.

Differential scanning calorimetry (DSC) was performed on a Netzsch DSC 204 with CC 200 liquid nitrogen cooling system to determine the glass transition temperatures ( $T_g$ ), and thermogravimetric analysis (TGA) of the obtained polymers were performed on a PL TGA 1500 instrument to determine thermal degradation. For DSC analysis, samples were heated from -50 to +300°C in a nitrogen environment at a rate of 10°C min<sup>-1</sup>. Figure 3 shows the thermogravimetric traces of the multigraft copolymers. Thermal analysis results are given in Table IV.

Swelling degrees of polymers obtained at equilibrium were determined by gravimetry at room temperature in CHCl<sub>3</sub>. Swelling ratios,  $q_v$ , were calculated using the volume ratio of swollen polymer ( $v_{\text{swollen polymer}}$ ) to dry polymer ( $v_{\text{dry polymer}}$ ).<sup>42,43</sup> Swelling ratios of the crosslinked multigraft copolymers are listed in Table II.

**TABLE II**  
Results and Conditions of the Synthesis of the Multigraft Copolymers at 26°C

Multigraft copolymer	PLO <sub>s</sub> (g)	PSB <sub>s</sub> (g)	PLina <sub>s</sub> (g)	PHA-soya (g)	MMA (g)	Polym. time (h)	Polymer yield		
							Total (g)	Crosslinked <sup>a</sup> (wt %)	$q_v$ <sup>b</sup>
57-1 (PHA-PLO-PMMA)	1.0	–	–	0.5	3.0	24	1.71	75.1	24.3
58-1 (PHA-PSB-PMMA)	–	1.0	–	0.5	3.0	24	1.54	48.0	36.0
59-1 (PHA-PLina-PMMA)	–	–	1.0	0.5	3.0	24	1.71	–	–

<sup>a</sup> The rest of the percentage is soluble polymer.

<sup>b</sup> Swelling ratio of the cross-linked polymer (in CHCl<sub>3</sub>).

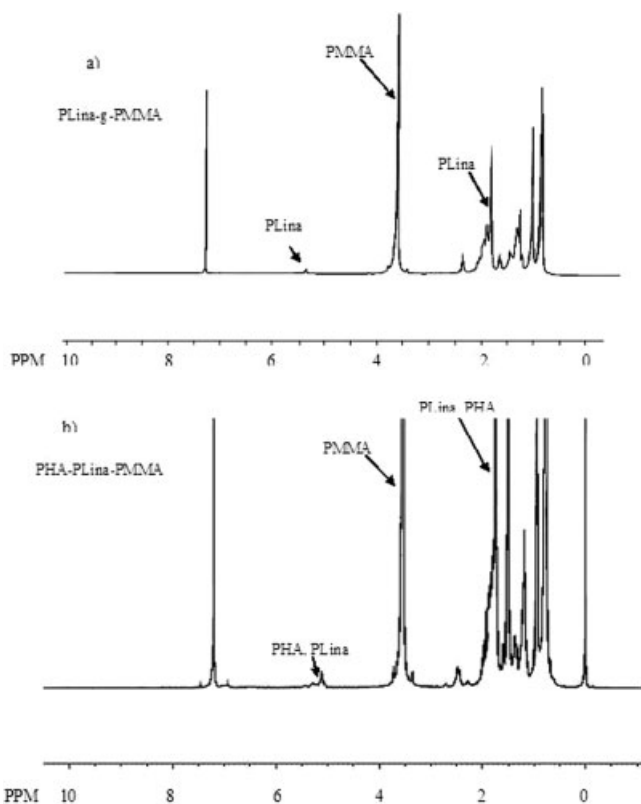


**Figure 1** <sup>1</sup>H NMR spectra of (a) the PLina-g-PMMA<sup>29</sup> and (b) PHA-PLina-PMMA copolymer samples (59-1).

For the protein adsorption tests, a Shimadzu UV 1601 model UV spectrophotometer was used.

**Tensile test**

For the polymer samples, the tensile tests are performed on AG-I 5 kN Shimadzu Autograph test machine with a constant tensile speed of 0.5 mm/min. The dimensions of the test specimens are given in Table V. In this table, the stress and strain values at break point of the three polymer specimens are presented. Figure 4 shows the stress-strain behavior of the specimens which are subjected to the above tensile test.

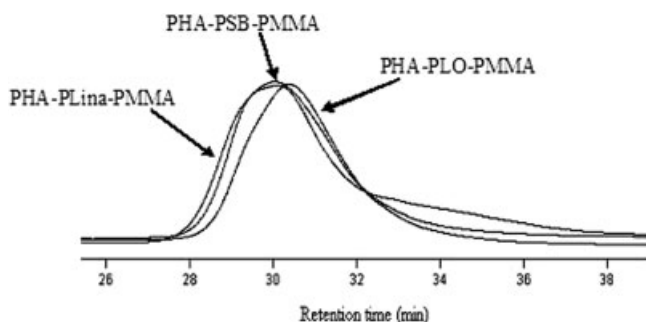


**Figure 2** GPC chromatograms of the fractional precipitated multigraft copolymers (57-1, 58-1, and 59-1).

**TABLE III**  
Copolymer Content and GPC Analysis of the Multigraft Copolymers

Run no	Molecular weight		Copolymer analysis (mol %)	
	$M_w (\times 10^4)$	MWD	PHA <sup>a</sup>	PMMA <sup>a</sup>
PHA-PLO-PMMA (57-1)	42.8	2.9	11	78
PHA-PSB-PMMA (58-1)	57.8	5.3	15	80
PHA-PLina-PMMA (59-1)	57.2	3.3	5	75

<sup>a</sup> From the TGA traces.

**Scanning electron microscope**

Scanning electron micrographs were taken on a JEOL JXA-840A electron microscope. The specimens were frozen under liquid nitrogen, then fractured, mounted, and coated with gold (300 Å) on an Edwards S 150 B sputter coater. The SEM was operated at 15 kV, and the electron images were recorded directly from the cathode ray tube on a Polaroid film. The magnification employed was varied up to  $\times 15,000$ ; however, 3000, 5000, 10,000, and 1000 magnifications were useful. SEM micrographs of the multigraft copolymers are shown in Figure 5.

**Human blood protein adsorption test**

Human albumin,  $\gamma$ -globulin, and fibrinogen were used to study the adsorption behavior of proteins on surfaces of polymer samples. Small disks (15 mm in diameter) of the polymer films were prepared using a punch and immersed in protein solutions containing 1 mg/mL of phosphate buffer solution (PBS) (pH 7.3–7.4) at

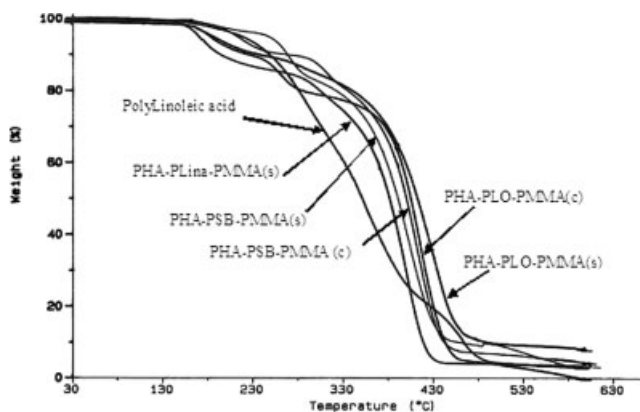


**Figure 3** Thermogravimetric traces of the PLina and multigraft copolymers/PLina: PHA-PLO-PMMA (soluble) (57-1), PHA-PLO-PMMA (crosslinked) (57-1), PHA-PSB-PMMA (soluble) (58-1), PHA-PSB-PMMA (crosslinked) (58-1), and PHA-PLina-PMMA (soluble) (59-1), multigraft copolymers.



**TABLE IV**  
**Thermal Analysis of the Multigraft Copolymers**

Polymer	DSC			TGA		
	$T_{g1}$ (°C)	$T_{g2}$ (°C)	$T_d$ (°C)	$T_{d1}$ (°C)	$T_{d2}$ (°C)	$T_{d3}$ (°C)
PMMA-PLO-PHA (soluble)	–	–	–	194	293	396
PMMA-PLO-PHA (crosslinked)	52	–	120	186	284	434
PMMA-PSB-PHA (soluble)	–	115	–	174	266	398
PMMA-PSB-PHA (crosslinked)	50	–	–	183	262	417
PMMA-PLina-PHA (soluble)	82	–	–	170	305	401

37°C for 1 h. The discs were then recovered and changes in the protein concentrations of the solution borne proteins were determined using an UV spectrophotometer.<sup>35,44</sup> The amount of adsorbed protein on the copolymer surface was calculated as follows:

$$\text{AAP}(\mu\text{g}/\text{mL}) = 1.55 \times \text{APS}(\lambda = 280 \text{ nm}) - 0.76 \times \text{APS}(\lambda = 260 \text{ nm}) \quad (1)$$

where AAP is the amount of adsorbed protein and APS is the absorbance of protein solution.

Amount of adsorbed protein on the copolymer surface was calculated from the difference between UV absorbency of a standard solution and that of the solution after the polymer disc was removed (each experiment was repeated seven times).<sup>29</sup> Obtained values for AAP were divided by disk area ( $\mu\text{g}/\text{cm}^2$ ). Results of adsorption measurements of albumin,  $\gamma$ -globulin, and fibrinogen on the prepared PMMA and copolymer disc surfaces are listed in Table VI.

### Bacterial adherence

One *Staphylococcus epidermidis* and one *Escherichia coli* isolates obtained from two different patients who had infections related to intravascular and urinary catheters were used for the adherence tests. The bacteria were kept frozen at  $-80^\circ\text{C}$  in skim milk. Ten microliters of the bacterium culture was inoculated onto a blood agar plates (Oxoid, UK); tryptone (14.0 g/L), peptone (4.5 g/L), yeast extract (4.5 g/L), sodium chloride (5.0 g/L), agar (12.5 g/L), and sheep blood (7 wt %), and kept overnight at 37°C. Bacterial suspensions of  $10^8$  colony forming unit (CFU) per mL were prepared for each bacterium for the adherence tests according to the method in cited Refs. 45–47. For this

purpose, polymer disc (thickness  $\sim 1$  mm,  $\phi = 6$  mm) was placed under sterile conditions in 1 mL of bacterial suspension and incubated at 37°C for 30 min. Polymer disc was removed and rinsed with 2 mL sterile PBS three times for 60 s to eliminate nonadhering bacteria. The polymer disc was then transferred into 1 mL of PBS in glass tube and agitated for 3 min via vortex at 2400 rpm/min. A 10  $\mu\text{L}$  sample of PBS containing dislodged bacteria was seeded on blood agar plates and spread to facilitate subsequent colony counting. Tenfold dilutions were made to calculate an accurate count of bacteria adhered to the polymer disc surfaces. Tenfold-dilutions colonies were counted by the naked eye after 24 h of incubation at 37°C. The bacterial density per polymer type (CFU/mL/ $\text{mm}^2$ ) was calculated by dividing the colony number mean by the total surface area ( $\text{mm}^2$ ) of the polymer disc. Results of the bacterial adhesion on the multigraft copolymers by direct counting of viable adherent bacteria are released by vortex agitation. The bacterial density (CFU/mL/ $\text{mm}^2$ ) was calculated by dividing the colony number mean by the total surface area of the polymer disc.

## RESULTS AND DISCUSSION

Medium chain length (mcl) PHAs may be elastomeric but have very low mechanical strength. Therefore, for packaging materials, biomedical applications, tissue engineering, and other specific applications, the physical and mechanical properties of microbial polyesters need to be diversified and improved.<sup>19</sup> PMMA is an acrylic hydrophobic biostable polymer that is widely used in the biomedical field as bone cement in orthopedics and traumatology and as implant carrier for sustained local delivery of antiinflammatory or anti-

**TABLE V**  
**Dimensions of the Tensile Test Specimens and Test Data**

	Thickness (mm)	Width (mm)	Gauge length (mm)	Stress at break ( $\text{N}/\text{mm}^2$ )	Strain at break (%)
PMMA	0,2150	5	15	12.5	34
PLina-g-PMMA (67-2)	0.05	5	15	55	30
PHA-PLina-PMMA (59-1)	0.05	5	15	48	9

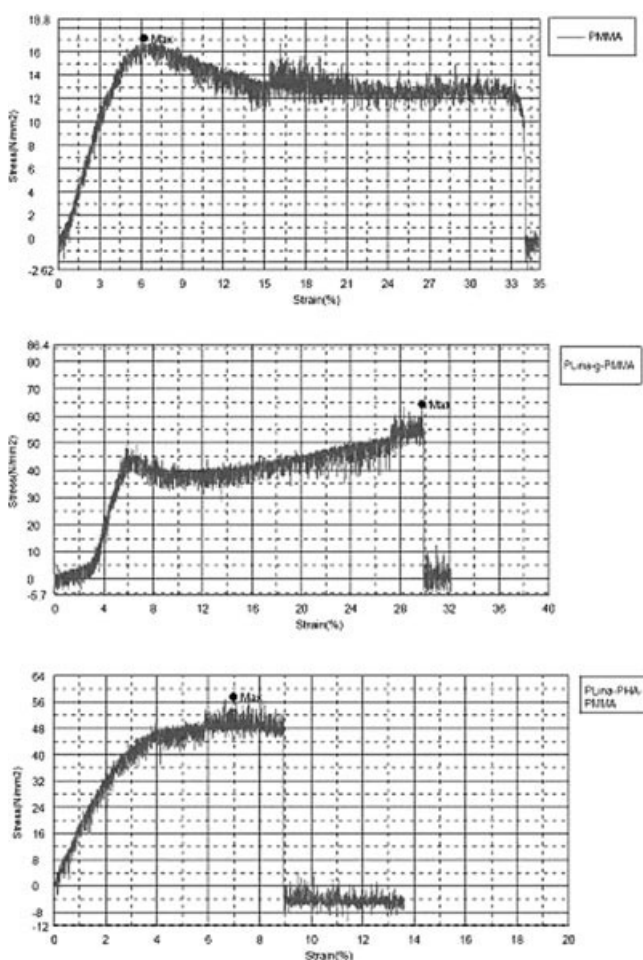


Figure 4 Stress-strain curves for tested polymers.

otics drugs.<sup>48</sup> The presence of oil/fatty acid chain in the polymer structure improves some physical properties of polymer in terms of flexibility, adhesion, resistances of water and chemicals. Because of their source and structural nature, triglyceride oils can widely be used as themselves. In bioapplications their biocompatibility and/or biodegradability play an important role.<sup>49</sup>

Autooxidation of the oils and linoleic acid caused the formation of polymeric oil/oily acid peroxides (sPLO, sPSB, and PLina), which were characterized by means of molecular weight measurements and the peroxygen analysis (see Table I). Molecular weights of the polymeric peroxides were changing between from 1684 to 4690 Da. Peroxygen content of the polymeric peroxides were found between from 0.66 to 1.32. So, these macroperoxy initiators were successfully used to initiate free radical polymerization of methyl methacrylate. Scheme 1 explains the simple design of the graft copolymerization mechanism. In this manner, polymeric oil/oily acid peroxide produces polymeric oil/oily acid radicals, which can both initiate the polymerization of MMA and attack to the double bonds of PHA.<sup>22</sup>

In this work, free radical polymerization of MMA was initiated by each polymeric oil/oily acid peroxide initiator in the presence of PHA to give partly cross-linked PMMA-PLO-PHA and PMMA-PSB-PHA multigraft copolymers, and completely soluble PMMA-PLina-PHA multigraft copolymers. Results and conditions of the graft copolymerization are listed in Table II.

Crosslinked and soluble copolymer fractions were isolated by means of chloroform extraction. Swelling degrees of the crosslinked multigraft copolymers at equilibrium indicated that the crosslinking density is low (e.g.,  $q_v = 24.3$  and  $36.0$ ).

Soluble fractions of the multigraft copolymers were fractionally precipitated to determine the  $\gamma$  values of the graft copolymers. Homo-PHA and homo-PMMA precipitated in the  $\gamma$  ranges of 1.4–2.2 and 2.8–4.1 respectively, while homo-PLO, homo-PSB, and homo-PLina were soluble in chloroform-methanol mixture

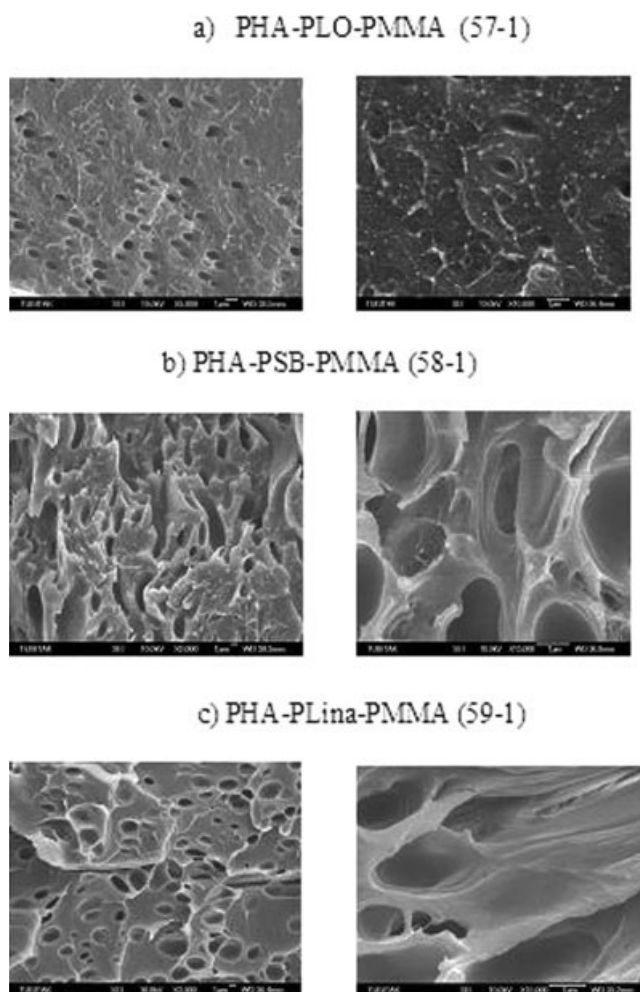


Figure 5 SEM micrographs of the multigraft copolymers: (a) PHA-PLO-PMMA (57-1) (left:  $\times 5000$  and right:  $\times 10,000$ ), (b) PHA-PSB-PMMA (58-1) (left:  $\times 3000$  and right:  $\times 15,000$ ), (c) PHA-PLina-PMMA (59-1) (left:  $\times 3000$  and right:  $\times 15,000$ ).

TABLE VI  
Protein Adsorption Results on the Multigraft Copolymers

Polymer	Albumin ( $\mu\text{g}/\text{cm}^2$ )	$\gamma$ -Globulin ( $\mu\text{g}/\text{cm}^2$ )	Fibrinogen ( $\mu\text{g}/\text{cm}^2$ )	Reference
PMMA	7.1	3.1	20.7	16
PLO-g-PMMA (run no: 39-6)	2.7	2.3	19.4	16
PHA-PLO-PMMA (run no: 57-1)	6.4	3.3	19.6	This work
PSB-g-PMMA (run no: 56-5)	4.6	3.1	20.1	16
PHA-PSB-PMMA (run no: 58-1)	4.4	3.5	19.8	This work
PLina-g-PMMA (run no: 67-1)	0.0	0.0	0.0	16
PHA-PLina-PMMA (run no: 59-1)	3.0	3.7	19.6	This work

( $\gamma > 10$ ). However, PLO-PHA-PMMA, PSB-PHA-PMMA, and PLina-PHA-PMMA multigraft copolymer fractions precipitated in  $\gamma$  values of 0.4–2.0 and 2.0–4.0, respectively. Because  $\gamma$  values of the multigraft copolymers with PMMA and PHA-homopolymers were almost superimposed, fractional precipitation was useful only in determining the  $\gamma$  values of the multigraft copolymers instead of isolating pure graft copolymers from the related homopolymers except unreacted polymeric oil/oily acid. Homo-PLO, -PSB, and -PLina, pale yellow liquids, were already eliminated by staying in the solution during the precipitation procedure. As we will discuss later, unimodal GPC curves can be attributed to the pure graft copolymers freed from the related homopolymers.

$^1\text{H}$  NMR spectra of the soluble multigraft copolymer samples contained the characteristic peaks of PMMA  $-\text{COOCH}_3$  at 3.7 ppm, PHA  $-\text{CH}-\text{O}-$  at 5.2–5.4 ppm, and the peaks of the triglyceride  $-\text{CH}-\text{O}-$ ,  $\text{CH}_2-\text{O}-$  at 4.1–4.4 ppm. Typical  $^1\text{H}$  NMR spectra of the PLina multigraft copolymer and PLina-g-PMMA diblock/graft copolymer are shown in Figure 1. The characteristic signals of the additional PHA blocks were observed in  $\delta$ : 1.0–2.0 and 5.0–5.4 ppm.

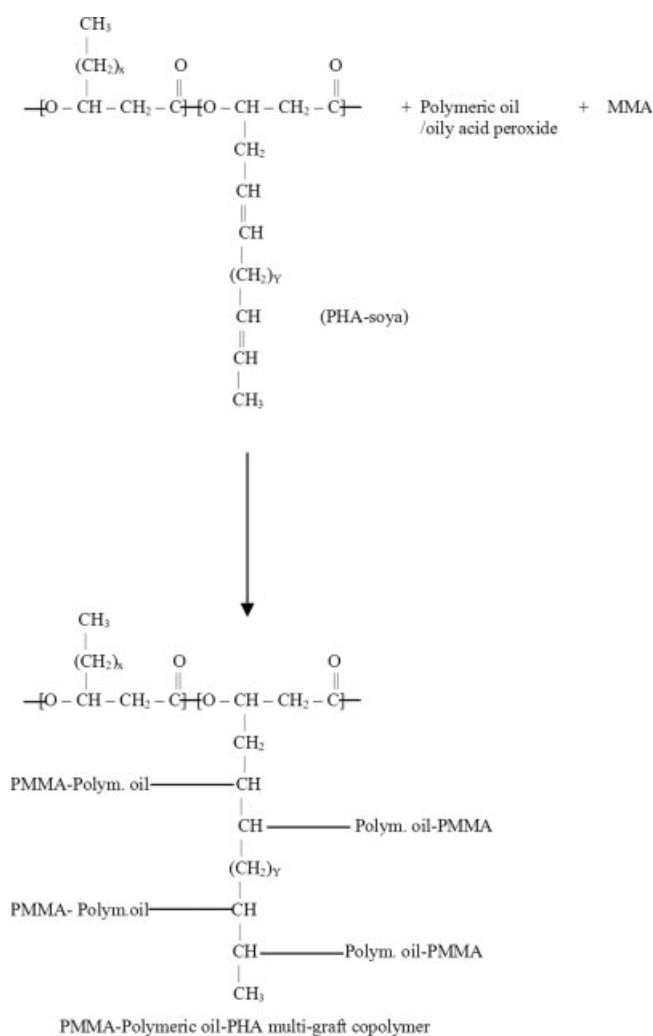
GPC was used to determine the molecular weights and polydispersity of the fractionated multigraft copolymers (see Table III). GPC chromatograms of the graft copolymers were all unimodal as shown in Figure 2, which can be attributed to the pure multigraft copolymer samples.

Thermal analysis of the graft copolymers was performed by DSC and TGA. Table IV lists the glass transition ( $T_g$ ) and decomposition temperature ( $T_d$ ). PHA and polymeric oils caused the plasticizer effect and it is observed that  $T_g$  of multigraft polymer decreased to  $50^\circ\text{C}$  where  $T_g$  of homo PMMA is  $\sim 105^\circ\text{C}$ . We have also observed peroxide decompositions in the same sample at around  $115^\circ\text{C}$ . In TGA curves, the graft copolymers have three decomposition steps: decomposition at  $170$ – $190^\circ\text{C}$  may come from the peroxide decomposition of the undecomposed peroxide groups of polymeric oil peroxides.  $285$ – $300^\circ\text{C}$  belongs to the decomposition of the PHA blocks and  $T_d$  around  $400^\circ\text{C}$  belongs to the PMMA and polymeric oil blocks.

Copolymer analysis was performed using the TGA curves. Thus, PHA content in the graft copolymer was calculated in a range from 5 to 15 mol % (see Table III).

### Tensile test

In Table V and Figure 4, the stress and strain values at break point of the three polymer specimens are presented. When the graphs are observed, PMMA has ~



Scheme 1 Formation of the multigraft copolymers.



12.5 MPa stress at break point and 34% strain at break point. It is worth noting that the data for PMMA may show discrepancies with the data given in the literature because these properties are highly dependent on the tacticity of PMMA. Containing PLina in its structure, PLina-*g*-PMMA copolymer has increased values for the stress at its break point (55 MPa), more or less preserving the strain value at its break point (30%) when compared to PMMA. However, for the PHA-PLina-PMMA copolymer, which contains both PLina and PHA, the strain at break point is reduced up to ~9%, more or less preserving the high stress values at its break point (48%) when compared to PLina-*g*-PMMA.

### SEM analysis

SEM analysis showed the microstructure of the fractured surface of the copolymers obtained. Figure 5 indicates the SEM pictures of the copolymer samples of PHA-PLO-PMMA, PHA-PSB-PMMA, and PHA-PLina-PMMA. Homogeneous structure was observed for PHA-PLO-PMMA (sample 57-1), PHA-PSB-PMMA (sample 58-1), and PHA-PLina-PMMA (sample 59-1) copolymers where tiny holes are present within [see Fig. 5(a-c)].

### Human blood protein adsorption test

Polymeric materials, including pure polymers and copolymers, are extensively applied as biomedical materials. The biocompatibility of a polymeric material can be inferred by studying the protein adsorption on the polymer. After a polymeric material is implanted, the first body reaction is protein adsorption which is an undesired effect. However, the treatment of hypoproteinemia requires the purification of albumin. Because of aforementioned reasons, it is crucial to know the protein adsorption behavior of the polymeric materials used as biomaterials. Surface morphology and surface chemical structures can also mediate protein adsorption behavior. Results of protein adsorption measurements with albumin,  $\gamma$ -globulin, and fibrinogen onto the prepared samples are shown in Table VI.

Less amount of albumin,  $\gamma$  globulin, and fibrinogen adsorptions are observed for PLO-*g*-PMMA, PSB-*g*-PMMA, PLina-*g*-PMMA when compared to PMMA. However, the albumin adsorption is reduced for the PHA containing multiblock copolymers when compared to PMMA while it is increased when compared to PLO-*g*-PMMA, PSB-*g*-PMMA, PLina-*g*-PMMA. On the other hand,  $\gamma$ -globulin adsorption of the PHA containing multiblock copolymers is increased when compared with PMMA and PLO-*g*-PMMA, PSB-*g*-PMMA, PLina-*g*-PMMA. For fibrinogen adsorption, the values for PHA-PLO-PMMA and PHA-PLina-

PMMA are reduced compared with PMMA while they are increased when compared to PLO-*g*-PMMA and PLina-*g*-PMMA, but values for PHA-PSB-PMMA are lower than those which are measured for both PMMA and PSB-*g*-PMMA.

These results showed that PLO, PSB, PLina, and PHA blocks affect the mechanical strength and ductility of copolymers and play an important role in decreasing the adsorption of protein.

### Bacterial adherence

Bacterial adherence to polymer surfaces varied significantly depending on the polymer type as well as the strain of the bacteria.<sup>37</sup> There are many studies involved in bacterial adhesion on different polymer surfaces.<sup>50-52</sup> The factors involved in the initial adhesion of bacteria to a substrate can be explained in terms of nonspecific interactions (electrostatic forces, hydrogen bonds, and Van der Waals forces) and hydrophobic interactions. Van der Waals forces which are usually attractive, come in to play at a separation distance (between bacteria the repellent electrostatic forces increase due to an overlap of the electron clouds of both bacteria and surface) of  $\geq 50$  nm and hold the bacteria relatively weakly to the surface.<sup>53-55</sup> At a separation distance of about 10-20 nm, the bacterial cell, although weakly held, is kept away from the substrate surface by electrostatic repulsion forces. At  $\leq 2$  nm, water adsorbed to bacteria or substrate surfaces can act as a barrier to bacterial attachment. The exclusion of water to enable attachment is not kinetically favorable; hydrophobic interactions, however, if present (usually within 2 nm of the surface) can help exclude water through nonpolar regions on both surfaces. Once a separation of  $\leq 1$  nm is reached, other adhesion forces such as ionic bridging, hydrogen bonding, and ligand-receptor interactions occur.<sup>56,57</sup>

In this study, the adherence of bacteria to copolymer PMMAs was compared with that of PMMA. One *S. epidermidis* and one *E. coli* to the PMMA and graft copolymers were used for the adherence tests. While the bacterial adhesion on PMMA for *S. epidermidis* and *E. coli* were the same, with insertion of PLO and PSB to PMMA, bacterial adhesion decreased significantly for *E. coli* (100- and 300-fold respectively) and *S. epidermidis* (twofold for each). Insertion of PLina did not affect *E. coli* adhesion when compared with PMMA, but *S. epidermidis* adhesion increased ~ 45-fold. PHA insertion to grafts, adhesion of both bacteria was increased significantly but this increment was higher for *E. coli* than for *S. epidermidis*. PHA insertion to PLO-PMMA and PSB-PMMA grafts increased the bacterial adhesion for *S. epidermidis* ~ 70- and 207-fold, respectively, while insertion of PHA to PLina-PMMA resulted in twofold increase. With the PHA insertion to PLO-PMMA, PSB-PMMA, and PLina-PMMA



**TABLE VII**  
**Results of the Bacterial Adhesion on the Multigraft Copolymers**

Polymer	<i>S. epidermidis</i>	<i>E. coli</i>	References
PMMA	46,000	43,000	15
PLO-g-PMMA(39-6)	27,000	428	This work
PMMA-PLO-PHA (57-1)	1,900,000	110,000	This work
PSB-g-PMMA (56-5)	28,000	132	15
PMMA-PSB-PHA (58-1)	5,800,000	190,000	This work
PLina-g-PMMA (67-2)	2,100,000	43,000	This work
PMMA-PLina-PHA (59-1)	4,200,000	160,000	This work

Determined by direct counting of viable adherent bacteria released by vortex agitation ((CFUs/mL)/mm<sup>2</sup>). The bacterial density ((CFUs/mL)/mm<sup>2</sup>) was calculated by dividing the colony number mean by the total surface area of the polymer disk.

grafts, bacterial adhesion increased 257-, 1439-, and 3-, 7-fold respectively, for *E. coli* (Table VII). Very few microbes have purely hydrophobic or charged surfaces. Their surfaces are complex, possessing charged residues as well as hydrophobic residues.<sup>58</sup> It can be concluded adhesion of bacteria on pure linoleic acid is much higher than the triglycerides. As explained above, hydrophobic interactions contribute to the initial adhesion of microorganism to surfaces and concordant with this finding, in our study, PHA insertion to whole binary grafts resulted in increased bacterial adhesion. Even though more hydrophobic grafts with insertion of PLO and PSB to PMMA have been obtained, bacterial adhesion on that grafts (especially for *E. coli*) decreased independently from the polymer hydrophobicity.

## CONCLUSIONS

As macro-peroxyinitiators, PLO, PSB, and PLina initiate the free radical polymerization of the unsaturated PHA and synthetic MMA and biodegradable and biocompatible multiblock copolymers are obtained by altering the properties of monomers. Diversification of the biomaterials can be diversified by using edible oils. This can be done in two ways, either by direct synthesis of the polymeric peroxides via autooxidation or by obtaining polyesters from microorganisms. It is crucial to know the protein adsorption behavior and bacterial adherence of the polymeric materials to be used as biomaterials. Polymeric oil peroxides have antimicrobial properties and nonprotein adsorbability while microbial polyester, PHA, affects the bacteria adherence and protein adsorption. Thus, insertion of the PHA into the multigraft copolymers caused the dramatic increase in bacterial adhesion on the polymer surfaces. PHA insertion into the graft copolymers decreased the albumin and  $\gamma$ -globulin adsorption but increased the fibrinogen adsorption when compared

to PMMA. PLO, PSB, and PLina blocks affect the mechanical strength and ductility of polymers and play an important role in decreasing the adsorption of protein and bacterial adherence.

## References

1. Lenz, R. W.; Marchessault, R. H. *Biomacromolecules* 2005, 6, 1.
2. Steinbüchel, A.; Valentin, H. E. *FEMS Microbiol Lett* 1995, 128, 219.
3. Doi, Y. *Microbial Polyesters*; VCH: New York, 1990.
4. Hazer, B.; Lenz, R. W.; Fuller, R. C. *Macromolecules* 1994, 27, 45.
5. Curley, J. M.; Hazer, B.; Lenz, R. W.; Fuller, R. C. *Macromolecules* 1996, 29, 1762.
6. Hazer, B.; Lenz, R. W.; Fuller, R. C. *Polymer* 1996, 37, 5951.
7. Kim, Y. B.; Kim, D. Y.; Rhee, Y. H. *Macromolecules* 1999, 32, 6058.
8. Ritter, H.; Von Spee, A. G. *Macromol Chem Phys* 1994, 195, 1665.
9. Lageveen, R. G.; Huisman, G. W.; Preusting, H.; Ketelaar, P.; Eggink, G.; Witholt, B. *Appl Environ Microbiol* 1988, 54, 2924.
10. Scandola, M.; Focarete, M. L.; Adamus, G.; Sikarska, W.; Baranovska, I.; Szwierczek, S.; Gnatowski, M.; Kowalczyk, M.; Jedliński, Z. *Macromolecules* 1997, 30, 2568.
11. Gross, R. A.; De Mello, C.; Lenz, R. W.; Brandl, H.; Fuller, R. C. *Macromolecules* 1996, 22, 1106.
12. Ashby, R. D.; Foglia, T. A. *Appl Microbiol Biotechnol* 1998, 49, 431.
13. Hazer, B.; Torul, O.; Borcakli, M.; Lenz, R. W.; Fuller, R. C.; Goodwin, S. D. *J Environ Polym Degrad* 1998, 6, 109.
14. Eggink, G.; Van der Wal, H. M.; Huijberts, G. N.; De Waard, P. *Ind Crops Prod* 1993, 1, 157.
15. Van der Walle, G. A. M.; Huisman, G. J. H.; Weusthuis, R. A.; Eggink, G. *Int J Biol Macromol* 1999, 25, 123.
16. Majid, M. I. A.; Hori, K.; Akiyama, M.; Doi, Y. In *Biodegradable Plastics and Polymers*; Doi, Y., Fukuda, K., Eds.; Elsevier, B.V.: New York, 1994; pp 417.
17. Hazer, B. In *Biopolymers*; Steinbüchel, A., Ed.; Wiley-VCH: Weinheim, 2003; Vol. 10, p 181.
18. Hazer, B. *Curr Trends Polym Sci* 2002, 7, 131.
19. Hazer, B.; Steinbüchel, A. *Appl Microbiol Biotechnol* 2007, 74, 1.
20. Hazer, B.; Lenz, R. W.; Çakmakli, B.; Borcakli, B.; Kocer, B. *Macromol Chem Phys* 1999, 200, 1903.
21. Ilter, S.; Hazer, B.; Borcakli, M.; Atici, O. *Macromol Chem Phys* 2001, 202, 2281.
22. Çakmakli, B.; Hazer, B.; Borcakli, M. *Macromol Biosci* 2001, 1, 348.
23. Lu, Y.; Larock, R. C. *J Appl Polym Sci* 2006, 102, 3345.
24. Hazer, B. *J Polym Sci Part A: Polym Chem* 1987, 25, 3349.
25. Murty, K. S.; Kishore, K. *Macromolecules* 1996, 29, 4859.
26. Hazer, B.; Ayas, A.; Besirli, N.; Saltek, N.; Baysal, B. M. *Makromol Chem* 1989, 190, 1987.
27. Çakmakli, B.; Hazer, B.; Tekin, I. O.; Kizgut, S.; Koksall, M.; Menceoglu, Y. *Macromol Biosci* 2004, 4, 649.
28. Çakmakli, B.; Hazer, B.; Tekin, I. Ö.; Cömert, F. B. *Biomacromolecules* 2005, 6, 1750.
29. Çakmakli, B.; Hazer, B.; Tekin, I. Ö.; Açıkgöz, Ş.; Can, M. *J Am Oil Chem Soc* 2007, 84, 73.
30. Langer, R.; Vacanti, J. P. *Science* 1993, 260, 920.
31. Johnson, W. C.; Wang, J.; Chen, Z. *J Phys Chem B* 2005, 109, 6280.
32. Yavuz, H.; Duru, E.; Genc, O.; Denizli, A. *Colloids Surf A* 2003, 223, 185.
33. Bayramoglu, G.; Denizli, A.; Arica, M. Y. *Polym Int* 2002, 51, 966.
34. Tsai, W. B.; Grunkemejer, J. M.; Horbett, T. A. *J Biomed Mater Res* 1999, 130, 130.

35. Chung, C. W.; Kim, H. W.; Kim, Y. B.; Rhee, Y. H.; *Int J Biol Macromol* 2003, 32, 17.
36. Tunney, M. M.; Gorman, S. P.; Patrick, S. *Rev Med Microbiol* 1996, 7, 195.
37. Ishihara, K. *Trends Polym Sci* 1997, 5, 401.
38. Chen, J.; Soucek, M. D.; Simonsick, W. J.; Celikay, R. W. *Polymer* 2002, 43, 5379.
39. Codex Alimentarius FAO-WHO Food Standards Program, FAO. Rome, 2 Auflage, Band 8–1992<sup>2</sup>. Codex Standard für Sojaspeiseöl<sup>3</sup>.
40. Hazer, B.; Baysal, B. M. *Polymer* 1986, 27, 961.
41. Hazer, B.; Erdem, B.; Lenz, R. W. *J Polym Sci A: Polym Chem* 1994, 32, 1739.
42. Hamurcu, E.; Baysal, B. M. *Polymer* 1993, 34, 5163.
43. Yıldız, U.; Hazer, B. *Macromol Chem Phys* 1998, 199, 163.
44. Henry, J. B. *Clinical Diagnosis and Management by Laboratory Methods Protein Detection and Quantization, Specific Proteins*, 20th ed.; W. B. Saunders Company: Philadelphia, PA, 2001; Chapter 13, pp 249–263.
45. Isenberg, H. D. In *Clinical Microbiology Procedures Handbook*; Isenberg, H. D., Ed.; ASM: Washington, DC, 1992; Vol. 1, p 15.9.3.
46. Das, T.; Sharma, S.; Muralidhar, A. V. *Endophthalmitis Res Group J Cataract Refract Surg* 2002, 28, 703.
47. García-Saénz, M. C.; Arias-Puente, A.; Fresnadillo-Martinez, M. J.; Matilla-Rodriguez A. *J Cataract Refract Surg* 2000, 26, 1673.
48. Elvira, C.; Fanovich, A.; Fernandez, M.; Fraile, J.; Roman, J. S.; Domingo, C. *J Controlled Release* 2004, 99, 231.
49. Guner, F. S.; Yağcı, Y.; Erciyas, A. T. *Prog Polym Sci* 2006, 31, 633.
50. Speranza, G.; Gottardi, G.; Pederzoli, C.; Lunelli, L.; Canteri, R.; Pasquardini, L.; Carli, E.; Lui, A.; Maniglio, D.; Brugnara, M.; Anderle, M. *Biomaterials* 2004, 25, 2029.
51. Kodjikian, L.; Burillon, C.; Chanloy, C.; Bostvironnois, V.; Pellon, G.; Mari, E.; Freney, J. J.; Roger, T. *Invest Ophthalmol Visual Sci* 2002, 43, 3717.
52. Pinna, A.; Zanetti, S.; Sechi, L. A.; Usai, D.; Falchi, M. P.; Carta, F. *Ophthalmology* 2000, 107, 1042.
53. Derjaguin, B. V.; Landau, L. *Acta Physicochim* 1941, 14, 633.
54. Verwey, E. J. W.; Overbeck, J. T. G. *Theory of the Solubility of Lyophobic Colloids*; Elsevier: Amsterdam, 1948.
55. Fletcher, M. *Bacterial Adhesion, Molecular and Ecological Diversity*; Wiley-Liss: New York, 1996; p 89.
56. Rose, S. F.; Okere, S.; Hanlon, G. W.; Lloyd, A. W.; Lewis, A. L. *J Mater Sci Mater Med* 2005, 16, 1003.
57. An, Y. H.; Friedman, R. J. *J Biomed Mater Res (Appl Biomater)* 1998, 43, 338.
58. Doyle R. D. *Microbes Infect* 2000, 2, 391.